Fusion Engineering and Design 219 (2025) 115281

Contents lists available at ScienceDirect

Fusion Engineering and Design

journal homepage: www.elsevier.com/locate/fusengdes

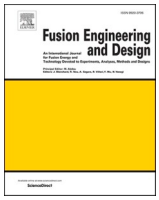

Thermo-structural assessment of the limiter inboard first wall design of the Divertor Tokamak Test facility

Riccardo De Luca [a,*], Maurizio Furno Palumbo [a,b], Paolo Frosi [a], Gabriele De Sano [b,c], Matteo Iafrati [a], Gian Mario Polli [a,b], Bruno Riccardi [b], Selanna Roccella [a]

[a] ENEA, Nuclear Department 00044 Frascati, Rome, Italy
[b] DTT S.c. a r.l, Via E. Fermi 45, Frascati 00044, Italy
[c] University of Rome Tor Vergata, Industrial Engineering Department, Via del Politecnico 1 00133 Rome, Italy

ARTICLE INFO

Keywords:
DTT
Power exhaust
Limiter
Plasma-facing components
Finite element
Thermo-structural assessment

ABSTRACT

The Divertor Tokamak Test facility (DTT) aims at investigating integrated power exhaust solutions that can be relevant for DEMO and future power plants. Such an ambitious goal imposes several constraints on the engineering design of the actively cooled plasma-facing components (PFCs) of DTT. For instance, the First Wall (FW) must withstand thermal and electromagnetic loads that arise during both normal and off-normal operations of various plasma scenarios. In particular, the Limiter Inboard FW (LIFW), covering 50 % of the IFW, has been designed to cope with plasma limited configurations, i.e. when the plasma interacts with the solid wall. Each module consists of seven long (2.3 m) coaxial pipes made of CuCrZr alloy. Owing to the high heat loads expected, the LIFW PFCs are based on the ITER-like W-monoblock design and the plasma-facing surface, protruding radially towards the plasma with respect to the standard IFW, has a toroidal shaping that helps distribute evenly the heat load. In the present work, the technological limits of the proposed LIFW design are assessed. Based on the hydraulic conditions of the cooling water, the maximum power that can be handled by the LIFW system is evaluated under the assumption of a safety margin from the critical heat flux (CHF). Moreover, the thermo-structural behavior of a LIFW unit is simulated in ANSYS under realistic boundary conditions. In this context, a parametric distribution of the thermal load is modelled as a function of the input power and the expected spatial-temporal evolution of the plasma "footprint". Moreover, realistic kinematic boundary conditions, representative of the pinned supports, have been included in the structural integrity assessment of the pipe, carried out according to the ITER SDC-IC design criteria (design-by-analysis approach). Preliminary results suggest that the maximum peak heat flux that can be handled by the LIFW design falls in the range 5–8 MW/m^2. This range is compatible with the DTT "Day0" scenario, when, due to the lesser knowledge of machine control, the most critical limiter operations may occur. Nonetheless, studies on the full power scenarios confirmed that in the ramp-up phase the maximum conductive heat load shall be lower than 1 MW/m^2 therefore the calculated performances can be considered adequately safe. After the fabrication of small-scale mock-ups, the lifetime of such components will be assessed experimentally, by means of cyclic thermal fatigue high heat flux tests.

1. Introduction

In the European Roadmap, controlling the heat and particle exhaust inside a tokamak is a key mission towards the realization of nuclear fusion [1]. In this context, the Divertor Tokamak Test facility (DTT) aims at investigating integrated power exhaust solutions that can be relevant for DEMO and future power plants [2]. DTT is a relatively compact device with a significant amount of heating power resulting in a high P/R ratio, in between the one of ITER and EU-DEMO. In addition, it must be operationally flexible and compliant with a number of plasma configurations. These requirements impose several constraints and challenges to the engineering design of the in-vessel components of DTT. For instance, the first wall (FW) must cope with thermal and electromagnetic (EM) loads arising during the various plasma scenarios, including normal and off-normal operations. Depending on the location inside the vacuum vessel, the FW modules are distinguished into Outboard, Top

* Corresponding author.
E-mail address: riccardo.deluca@enea.it (R. De Luca).

https://doi.org/10.1016/j.fusengdes.2025.115281
Received 13 January 2025; Received in revised form 5 May 2025; Accepted 14 June 2025
Available online 26 June 2025

and Inboard first wall (IFW). In its turn, the IFW is composed of 18 standard modules (SIFW) and 18 limiter modules (LIFW). DTT will be a tokamak operating with a fully actively cooled metallic wall with controlled temperature. In the existing tokamaks, above all JET as a representative tokamak also scalable to ITER, sacrificial limiters are envisaged to cope with plasma transients and to protect the otherwise unshadowed reactor wall from excessive damage [3]. Therefore, in view of DEMO, a reliable wall protection strategy involving sacrificial limiters is unavoidable, and it is indeed among the Key Design Issues to be addressed [4].

The limiter modules of DTT must prevent the standard modules from direct plasma-wall interaction during plasma limited phases, ramp-up/down, negative triangularity, plasma transients and accidents. For this reason, as shown in Fig. 1, each LIFW module covers 10° per sector, the remaining 10° being occupied by a SIFW module. In addition, the LIFW modules protrude radially towards the plasma with respect to the standard modules, and their plasma-facing surface has a toroidal shaping that helps spread more uniformly the heat when the plasma touches the solid wall. At this preliminary stage, the best shaping solution for the limiter is still under evaluation. Therefore, in the present work it was decided to simulate a simplified geometry where the shaped plasma-facing surface is not reproduced. Nonetheless, the effect of a proper toroidal shaping solution was considered in the applied heat load. This approach allows us to derive more generalized conclusions, which are valid for a properly shaped component.

A conceptual layout of a LIFW plasma-facing unit (PFU) was first delivered in 2021 [5,6]. It combines the robustness of the ITER-like W-monoblock design with the compactness of a CuCrZr coaxial pipe configuration as heat sink, due to the limited space available at the inboard side. Owing to the recent requirements coming from the supplier of the CuCrZr pipes, a layout variant was issued featuring the use of commercial pipes. In the new design, the outer pipe is characterized by the same outer diameter of 21 mm but increased thickness of 3 mm. In addition, the number of pinned supports and backplates for the fixation of the component to the vacuum vessel has increased up to 6 poloidal locations to better cope with the expected EM loads. The updated features of the LIFW design are summarized in Table 1. A single LIFW module gathers 7 coaxial pipes extending poloidally over a length of 2300 mm. Cooling water is provided at 4 MPa and 60 °C through port 1. The two feeding pipes reach a collector on each module (hydraulically connected in parallel with the other modules). The total mass flow rate available for the whole IFW is equal to 131 kg/s. Assuming a swirl tape in the external conduit of the coaxial layout, the resulting water velocity lies in the range 3.2–5.2m/s [7].

In the present work, the technological limits of the latest LIFW design are assessed through dedicated hydraulic and thermo-structural analyses carried out in MATLAB and ANSYS 19.1 under conservative but realistic boundary conditions. The ITER SDC-IC design criteria are employed for a preliminary assessment of the structural integrity of the component [8], ultimately providing a conservative estimation of the operating range of the LIFW design.

Table 1
Updated LIFW design features.

	Value	Unit
LIFW/IFW ratio	50	%
Number of pipes per module	7	
Inner pipe external diameter	15	mm
Inner pipe thickness	1.5	mm
Outer pipe external diameter	27	mm
Outer pipe thickness	3	mm
W block size width/height	35	mm
W monoblock axial thickness	30.6/12*	mm
Gap between monoblocks	1/0.4*	mm
Module poloidal length	2300	mm
Module mass	200	kg

*Related to the monoblock at a pinned support location.

2. Thermohydraulic analysis

As a first step, a routine was implemented in MATLAB R2024a to investigate the operating limits of the LIFW system under conservative assumptions on the load distribution over a properly shaped module. The routine provides a self-consistent calculation of the critical heat flux margin M_{CHF} within a broad range of the total power Q absorbed by the LIFW system of DTT during operation. The employed correlation reads

$$M_{CHF} = \frac{q_{CHF}}{f q_0} \geq 1.4 \quad (1)$$

where q_{CHF} is the critical heat flux (CHF) in MW/m^2, f is the heat flux peaking factor and q_0 is the design heat flux, in MW/m^2.

First of all, a series of input parameters must be provided to the MATLAB code, above all:

1. Characteristics of the LIFW system (monoblock geometrical features, available plasma facing surface and number of units per module, LIFW fraction at the inboard side or number of modules)
2. Water coolant properties (Total LIFW system mass flow rate, inlet pressure, inlet temperature, geometry of the conduit and twisted swirl tape in coaxial pipe configuration)
3. Heat flux peaking factor at the coolant, assumed on the base of monoblock geometrical considerations and verified with dedicated thermal simulations
4. Wall power density distribution under the assumption of a properly shaped plasma-facing surface

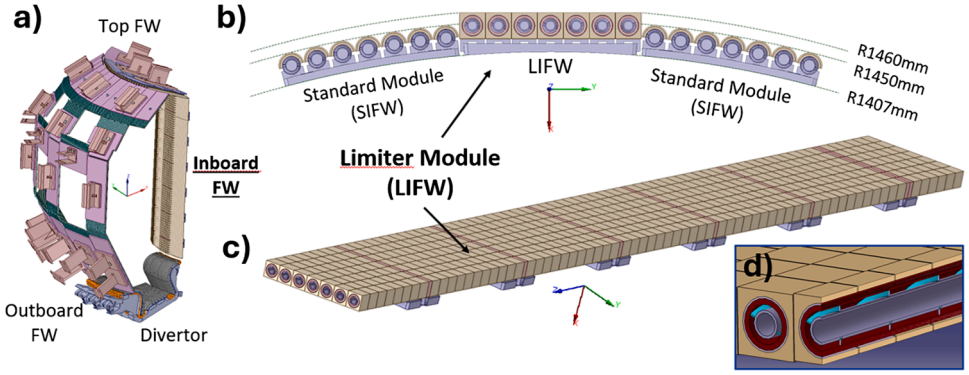

Fig. 1. a) DTT FW layout within a 30° toroidal section, with top view detail of the LIFW and SIFW modules at the inboard side covering 10° each b) and a detailed view of the LIFW model with the fixation structures c). d) Axial cross section view of a LIFW unit, where the coaxial pipes configuration and the swirl tape are shown. The solid model does not include the shaping of the plasma-facing surface.

In a second step, the design heat flux q_0 is correlated to the total absorbed power Q through the choice of a parametric wall power density distribution. Assuming a limited plasma operation with negligible radiation, the injected power is converted into the power delivered by the charged particles on the shaped plasma-facing surface of the LIFW system. The exponential decay of the power in the plasma region beyond the last closed flux surface (LCFS) is transferred to the solid wall leading to a characteristic profile with two symmetric peaks. The normalized wall profile is shown in Fig. 2 with respect to the poloidal direction (wall coordinate, in mm). By choice, the "zero" of the wall coordinate is where the LCFS is tangent to the solid wall. The employed profile is characterized by a single power decay length λ_q of 5 mm, in agreement with existing studies [9–12] and scaling laws [13,14] modeling the plasma edge transport of DTT during limited configurations. Consequently, the two symmetric peaks appear at approximately 90 mm from the point of tangency, and their width at maximum power is almost 33 mm. This procedure allowed us to establish a biunivocal correlation between the total power Q absorbed by the LIFW system and the corresponding peak heat flux q_0 at the wall. If needed, the choice of a different profile is also possible, and this would not affect the general validity of the established model. On the other hand, toroidal effects are neglected in the MATLAB routine. Above all, effects due to surface shaping, shadowing effects (e.g. of the surrounding limiters), installation tolerances and misalignments could have a strong impact on the power distribution on the limiter modules and must be considered. In this regard, dedicated research activities involving tools such as the line tracing code PFCflux are ongoing in support of the identification of the best shaping solution for the limiters of DTT.

As a third step, a conservative and self-consistent estimation of the CHF is obtained from the modified Tong-75 correlation [15] by including the effect of the water temperature increase as a function of Q. This effect is simply given by the power balance equation:

$$Q = mc_p(T - T_0) \tag{2}$$

where m is the mass flow rate, c_p is the temperature averaged specific heat and T_0 is the inlet water temperature. Similarly, the heat transfer coefficient (HTC) can be derived as a function of the pipe wall temperature through semi-empirical correlations that are specifically developed for the actively cooled PFCs employed in nuclear fusion devices [16].

Finally, Eq.(1) is employed to calculate the CHF margin within a broad range of absorbed power Q. By choice, the lower limit was set to Q = 8MW, which is compatible with the DTT "Day0" scenario, when, due to the lesser knowledge of machine control, the most critical limiter operations may occur. Nonetheless, studies on the full power scenarios confirmed that in the ramp-up phase the maximum conductive heat load shall be lower than 1 MW/m^2 therefore the calculated performances can be considered adequately safe [2]. The upper limit is imposed by the minimum acceptable value of the CHF margin depending on the thermo-hydraulic conditions of the cooling water. This allowed us to derive a conservative upper limit in a self-consistent way, depending on the absorbed power Q, the thermo-hydraulic characteristics of the cooling water, the chosen wall power density profile and the geometrical features of the limiter system.

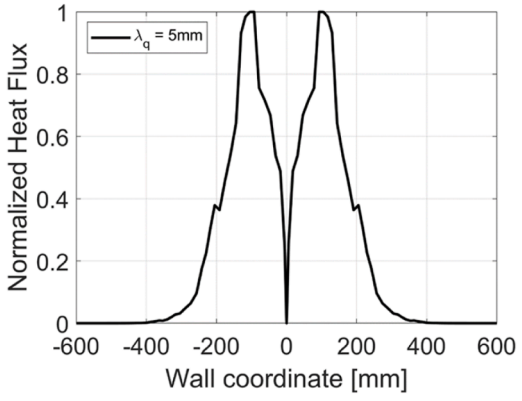

Fig. 2. Normalized wall power density profile in the poloidal direction. This profile features a single power decay length of 5 mm. The parametrization of this distribution established a biunivocal correlation between total power Q absorbed by the LIFW system and the maximum heat flux q_0 at the solid wall.

As shown in Fig. 3, for a given combination of water inlet temperature and velocity (pressure is 4 MPa), the CHF margin is obtained in a wide range of Q (see the lower x axis) or, correspondingly, in a wide range of q_0 (upper x axis). Considering the DTT-relevant FW water characteristics, namely 4 MPa, 3.2m/s and 60 °C at the inlet, the CHF margin reaches the limit of 1.4 at a value of Q_{lim} = 14MW, corresponding to a limit peak heat flux $q_{0,lim}$ = 10.4 MW/m^2.

Additional information related to the baseline scenarios is provided in Table 2. Higher margins in terms of Q_{lim} can be achieved, as expected, by reducing the inlet water temperature or by increasing the mass flow rate, and this routine can assess this effect in a quantitative way. For instance, in the blue curve of Fig. 3 the water velocity is increased to 5.2m/s leading in a shift of the Q_{lim} from 14MW to 19.1 MW ($q_{0,lim}$ = 14.5 MW/m^2); in the orange curve, the inlet temperature is reduced to 40 °C, again resulting in an increased Q_{lim} = 15.4 MW ($q_{0,lim}$ = 11.7 MW/m^2).

3. LIFW solid model and boundary conditions

As a further step, dedicated thermo-structural analyses were implemented in ANSYS Workbench 19.1 to assess the response of the LIFW under realistic boundary conditions. As shown in Fig. 4, a single PFU is modeled and meshed using less than 600,000 20-node-hex elements.

With respect to a complete coaxial pipe configuration, only the outer pipe is modelled and the presence of the inner pipe together with the swirl tape is taken into account in the HTC function applied to the nodes at the inner walls of the outer pipe. A detailed modeling of the collector at the upper end and the lower end of the PFU, where specific design solutions are foreseen to allow the correct water flow and distribution, is beyond the scope of this analysis, being covered in other published literature [7,17].

Realistic boundary conditions have been implemented in the finite

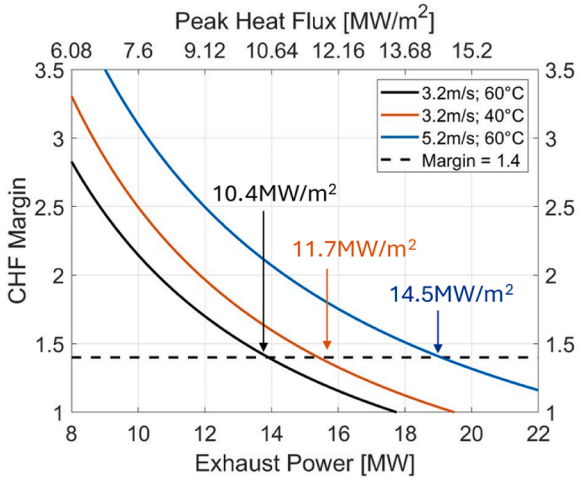

Fig. 3. Results of the thermohydraulic routine, providing the limits imposed by the cooling water characteristics in terms of power absorbed by the LIFW system (lower X axis) or peak heat flux of a given wall power density profile (upper X axis). The limit is imposed by a safety margin from the CHF equal to 1.4 and varies depending on the water characteristics. Water pressure is assumed to be 4 MPa.

Table 2
DTT baseline thermohydraulic results.

	DTT Day0	CHF Margin = 1.4	Unit
Absorbed power Q	8	14	MW
Peak heat flux q_0	6	10.4	MW/m^2
Peaking factor f	1.45	1.45	
Water pressure	4	4	MPa
Water inlet T	60	60	°C
Water outlet T	89.3	110.7	°C
Water velocity	3.2	3.2	m/s
HTC	35.18	39.05	kW/m^{2}K
CHF	24.93	21.5	MW/m^2
CHF Margin	2.83	1.40	

element model, as described hereafter. Considering the markers in Fig. 4a from the thermal point of view, the following boundary conditions are highlighted:

A. **Heat Transfer Coefficient (HTC):** applied to the nodes of the inner wall of the outer pipe as a function of the local temperature, according to semi-empirical correlations specifically developed for the actively cooled PFCs employed fusion applications [5]. DTT-relevant water conditions are assumed (4 MPa, 60 °C, 3.2–5.2m/s, swirl tape), which however result in a very modest value of the HTC, lower than 60kW/m^{2}K in forced convection.
B. **Parametric power density profile**: in addition to a uniform load, the profile described in the previous section (Fig. 2) was implemented in the ANSYS code to simulate plasma limited scenarios with heat loads varying in space and/or time. The "zero" of the distribution is on the monoblock at the fourth pinned support location. Therefore, the maximum load occurs after 90 mm from both the sides, and it is almost constant for a length of 33 mm. The choice of a different profile is possible and would not affect the global validity of the model.

Instead, by considering the markers of Fig. 4b from the structural point of view:

A. **Water pressure:** primary load of 4 MPa applied uniformly to the inner surfaces of the outer pipe.
B. **Nodal temperatures:** transferred from the thermal analysis results to the corresponding nodes of the structural mesh. Being the mesh identical, no interpolation is required. Temperatures are transferred from/to each body in the model.
C. **"Fixed" pinned support (UZ=UY=0)**: a set of kinematic constraints representative of a pinned support having hindered both the vertical displacement (UZ) and horizontal displacement (UY). This solution also prevents liabilities in the isostatic model. In addition, the rotation of the monoblock around the pin axis is allowed. This behavior is visible in Fig. 5, where the contour plot refers to the "-UY" displacement, namely the circumferential displacement with respect to the cylindrical coordinate system located at the axis of the pin hole. As desired, the color "bands" are equally spaced, and this confirms the linearity of the circumferential displacement with the distance from the pin axis
D. **Pinned support (UZ=0)**: set of kinematic constraints representative of a pinned support that hinders only the vertical displacement while keeping free the horizontal displacement and the rotation of the section around the pin axis as well, as shown in Fig. 5. This solution allows the pipe to expand in the horizontal direction without constraints, making the model isostatic.
E. **Symmetry (plane YZ)**

Material properties of the employed materials, namely Tungsten, CuCrZr alloy, AISI 316 L steel, OFHC Cu are tabulated in the document Appendix A – Material Design Limit Data of the ITER SDC-IC [8]. The plastic behavior of pure copper is simulated with a Chaboche kinematic hardening law valid from room temperature to 400 °C. Instead, the CuCrZr pipe has elastic properties for the structural verification in the elastic analysis approach.

4. LIFW thermo-structural assessment results

A second technological limit is imposed by the thermal stresses that arise in the component due to the developed temperature gradients as well as the stresses arising from having joined quite dissimilar materials. For this reason, thermo-structural simulations were carried out to assess the structural stability of a LIFW unit during normal operation. Despite the finite duration of a single plasma operation of DTT, lasting up to 100 s, this time is much larger than the time required by the actively cooled

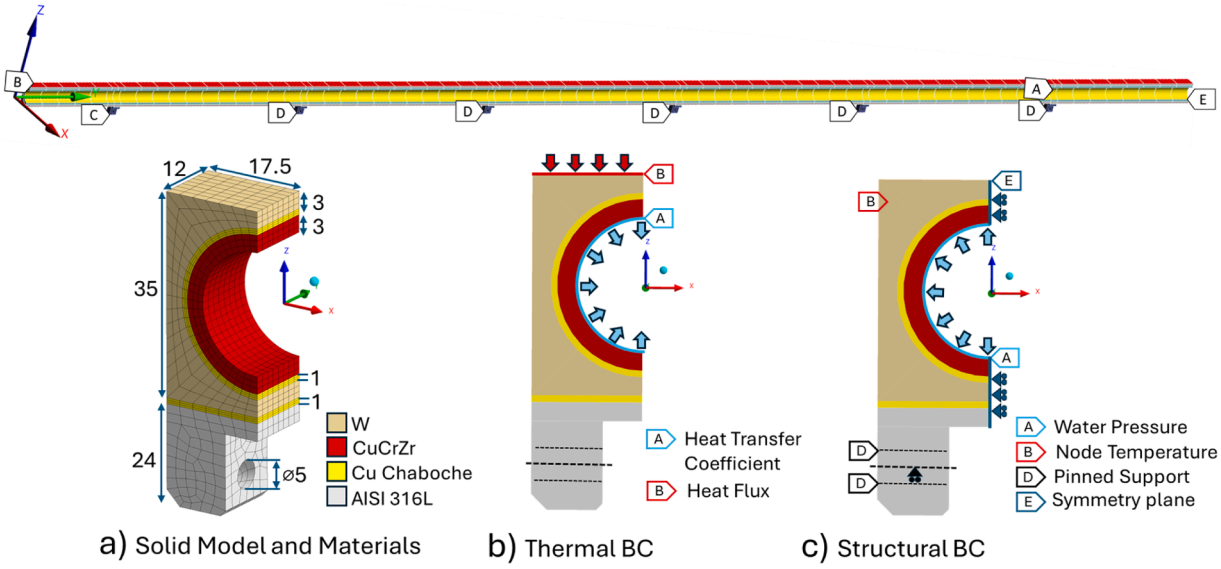

Fig. 4. Solid model of a single LIFW PFU, meshed in ANSYS 19.1 with <600,000 20-node-hex finite elements. a) Detail of the mesh at the location of a pinned support. Thermal and structural boundary conditions (BC) are respectively highlighted in b) and c) using markers, in detail: Heat transfer coefficient (HTC) and water pressure (A), heat load and nodal temperatures transferred to the whole domain (B), fixed support (C), pinned fixation (D) and symmetry plane (E).

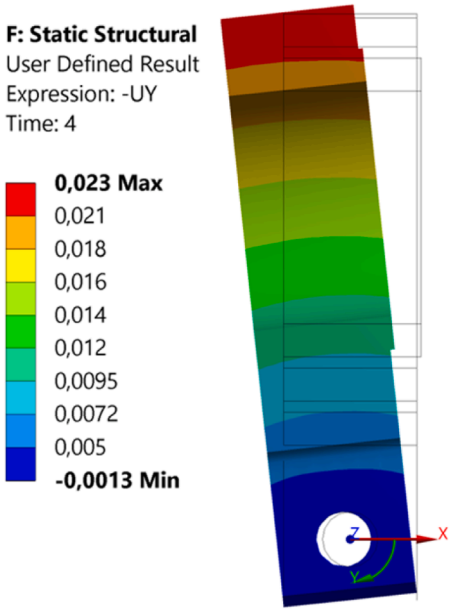

Fig. 5. Detail of a monoblock with pinned support. The contour plot shows the circumferential displacement -UY referred to the cylindrical coordinate system located at the axis of the pin hole. A set of kinematic boundary conditions replicates the behavior of the pinned joint: the vertical displacement is constrained, whereas the rotation around the pin axis is free. In the case shown here, the displacement along the pipe axis is also free, being hindered only at the fixed support (C).

PFC to reach the thermal equilibrium. For this reason, as described in the SDC-IC [8], structural integrity was verified with an elastic procedure, by simulating the worst instant of a full-power ramp-up phase of DTT with a steady state thermal analysis in ANSYS. This assumption is conservative and can be also representative of a number of limiter scenarios, instance limiter plasma pulses during the commissioning phase or negative triangularity operations. Both uniform and peaked heat flux profiles are investigated. In addition, the heat flux magnitude is scaled to replicate a range of the absorbed power Q up to 14MW, hence covering both the DTT-relevant cases mentioned in the previous sections with a substantial safety margin.

For brevity, in this section we report only on the results of a limited plasma operation with $Q = 14$ MW. In this case, the heat flux distribution is peaked, and the two maximum values in the loaded zone reach 10MW/m^2. The resulting temperature distribution, representative of the last part of the ramp-up phase or even a long limiter plasma configuration, is reported in Fig. 6. No criticalities are observed for the W block. In fact, the maximum temperature reached at the edges of the monoblock in the most loaded zone remains below 930 °C, owing to the optimized armour thickness of 3 mm, which keeps the temperature low, especially at the center of the monoblock. This temperature level is adequately lower than the temperatures at which the kinetic of recrystallization becomes significant, i.e. around 1200–1300 °C [17], so the recrystallization is not expected to be an issue for the proposed design. Fig. 7.

With respect to the CuCrZr outer pipe, in the loaded zone the maximum temperature nearly reaches 400 °C with Q equal to 14MW. Such a high value is similar to the maximum temperature reached by the CuCrZr pipe of the DEMO divertor target W-monoblock when the applied heat flux is 20MW/m^2. Although both the layouts are based on the W monoblock, it is interesting to notice the different behaviour. In DTT, the lower performances are primarily due to the available water conditions, which provide 3–5 times lower HTC in comparison with the DEMO-like divertor target water conditions [18]. Similarly, the different pipe geometry in the LIFW, with greater diameter and doubled thickness, plays a role in the reduction of the overall mechanical response. In the vector plot of Fig. 8, the heat flux absorbed by the water at the inner wall of the outer pipe is shown. The maximum value is on the high flux side, equal to 14.5MW/m^2 when the applied load is 10MW/m^2. This is due to the heat flux concentration at the pipe. Their ratio is the peaking factor, which was confirmed to be around 1.45, as expected.

In a second step, a static structural analysis was coupled with the steady state thermal analysis. As a first outcome, the deformation of the PFU during the operation is analyzed. In particular, the radial displacement, namely the Z displacement in the global coordinate system, should be minimized in the presence of a shaped plasma-facing surface, to avoid hot spots and leading edges. In Fig. 9, the contour plot of the radial displacement is provided on a model with strongly enhanced deformation for a better visualization of the small deviations from the original model (undeformed wireframe). It can be noticed that the imposed kinematic constraints keep the radial deformation below 0.36 mm. A final decision on the need to further reduce the radial displacement of the PFCs towards the plasma will be evaluated at the choice of the final toroidal shaping of each PFU of the LIFW module, to avoid the presence of hot spots and leading edges. As expected, the imposed kinematic constraints work properly, allowing pipe to freely expand along the Y direction (pipe axis). The contour plot in Fig. 10 shows the contour of the equivalent (Von Mises) stress arising in the loaded zone of the PFU. Despite the high values reached in the W blocks, stresses are localized and should not represent an issue for W, as it still offers a higher yield strength at the local average temperature. Instead, as highlighted in Fig. 11, the CuCrZr pipe experiences the unfavorable combination of high stresses and high temperatures, both occurring in the upper part of the pipe. In particular, the high temperature resonates in a significantly reduced maximum allowable stress.

The structural integrity of the pipe was preliminary assessed in a design-by-analysis way, by following the elastic analysis procedure described in the ITER SDC-IC [8]. Both the monotonic and cyclic level A

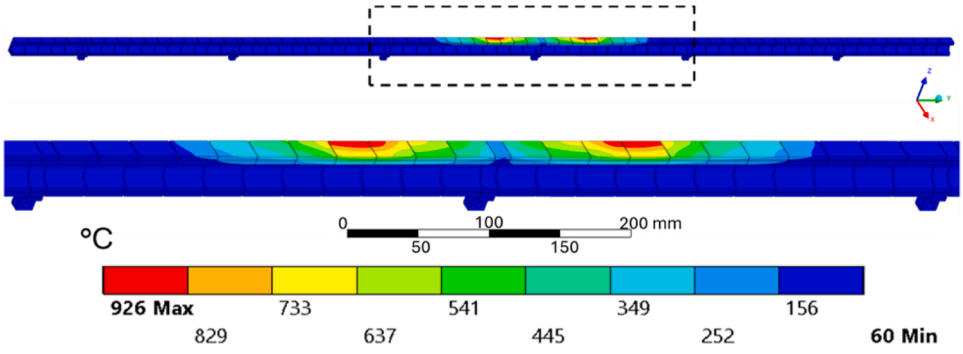

Fig. 6. Temperature distribution in the PFU, from a steady state thermal analysis of a plasma limited operation with 10MW/m^2 peak load. The maximum temperature of the W block remains below 930 °C.

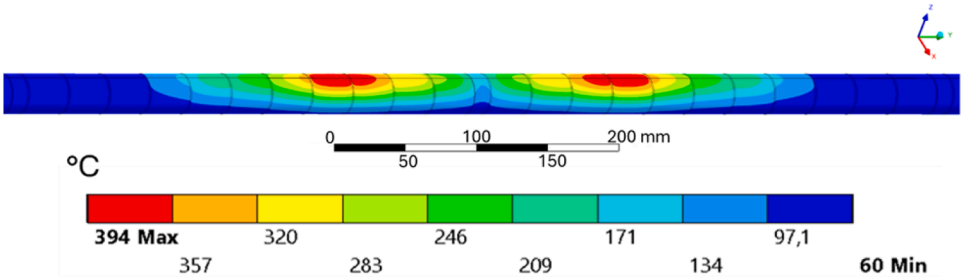

Fig. 7. Temperature distribution in the CuCrZr outer pipe during a plasma limited configuration with 10MW/m^2 peak load. The maximum temperature reached by the pipe is close to 400 °C. Results are visualized in the complete pipe body by using a visualization option of the symmetry plane elements.

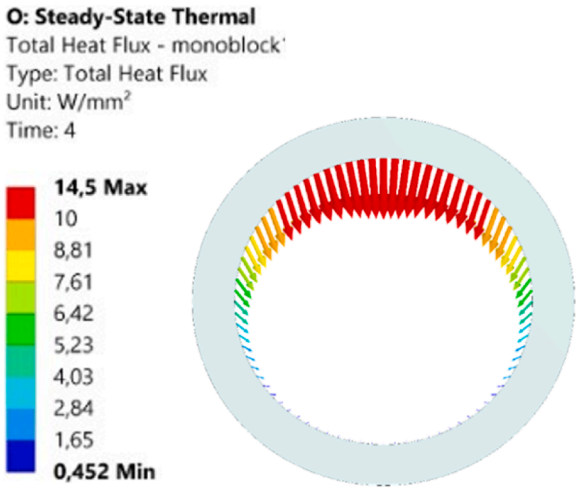

Fig. 8. Detail of the heat flux concentration at the upper part of the pipe wall, confirming a peaking factor around 1.45.

damage modes criteria have been addressed. However, being the secondary loads the main limiting factor of the lifetime of the PFCs, this section focuses on the description of the C-type low-temperature rule ("3Sm rule"). This criterion is verified if

$$K = \frac{(\overline{P_m + P_b})_{MAX} + \Delta[P+Q]_{MAX}}{3S_m\ (T_m, \Phi)} \leq 1 \tag{3}$$

where the upper term in the fraction is the maximum membrane plus bending stress intensity obtained by linearizing the stresses along a path through the thickness of the structural material in the most loaded zone. It has two contributions: $(\overline{P_m + P_b})_{MAX}$ is the membrane plus bending term due to primary loads (i.e. water pressure); $\Delta[P+Q]_{MAX} \sim \Delta[Q]_{MAX}$, the dominant term, is the maximum range of cyclic primary plus secondary stress intensities (mainly due to thermal gradients and material mismatch). In the lower part, the term $S_m\ (T_m, \Phi)$ is a characteristic maximum allowable stress of the structural material, tabulated in [8] as a function of the average path temperature T_m and neutron irradiation Φ.

Fig. 12 shows the five paths considered in this work for the stress linearization at two critical positions, called "peak" and "support" depending on their position in the loaded zone. The first one corresponds to the centre of the monoblock at the peak heat flux location; the second location refers to the monoblock with pinned support at the center of the loaded zone. According to the elastic analysis procedure, the structural pipe was modeled as a perfectly elastic material, and the verification is carried out against the linearized stresses from a static structural simulations.

Results listed in Table 3 indicate that the structural stability in Day0 operation is positively verified for all the paths of both the considered locations. On the other hand, at the higher heat flux of 10MW/m^2 the path AB in the upper part of the pipe exceeds the allowable limit by a significative amount. Despite this, all the other paths are positively verified. This result suggests the need for dedicated high heat flux tests, already foreseen after the fabrication of small-scale mock-ups, for a conclusive lifetime assessment.

The plots in Fig. 13 provide a generalized overview of the outcomes of the structural assessment. The blue curve gives the maximum linearized stress intensity along the critical path AB, outcome of the thermo-structural simulations. The "3Sm rule" criterion is verified as long as the blue curve remains below the maximum allowable stress limit $3S_m$ as a function of the average path temperature nd neutron fluence. In hte plots, the maximum allowable stress limit is provided by the yellow and orange curve depending on the characteristic treatment of CuCrZr, respectively "Tr.B" (solution annealing, cold working and ageing) and "Tr.A" (solution annealing and ageing).

In the baseline case of Fig. 13a, featuring a 3mm-thick pipe and

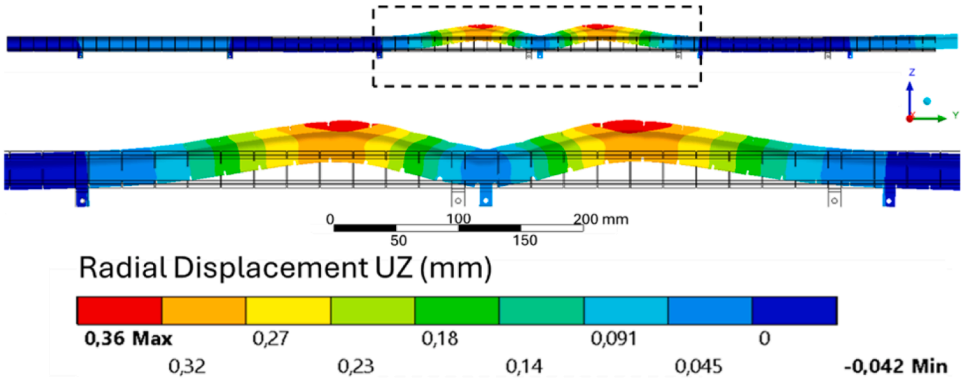

Fig. 9. Radial displacement (Z axis) of the PFU, visualized over a strongly deformed model (enhancement factor 85x) to appreciate the deviation from the undeformed model wireframe.

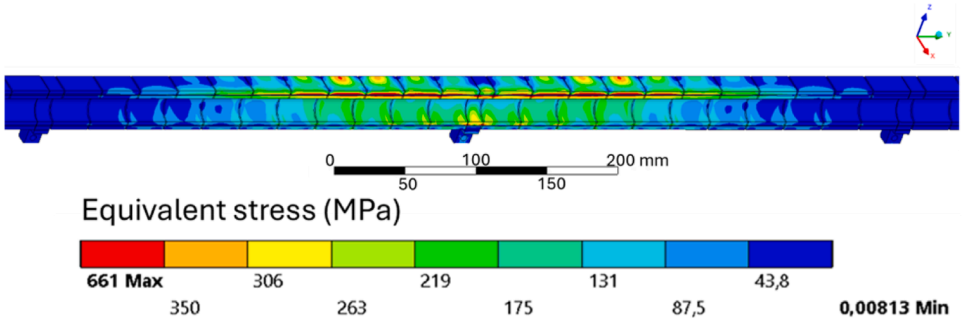

Fig. 10. Equivalent stress arising in the loaded zone of the PFU during plasma limited configuration with 14MW absorbed power (10MW/m^2 peak heat flux).

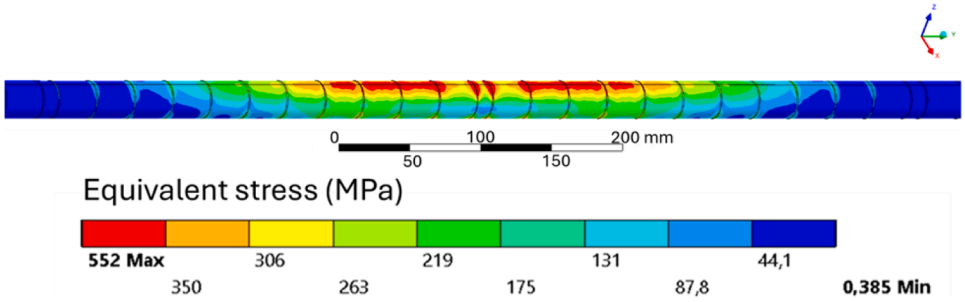

Fig. 11. Equivalent stress arising in the loaded zone of the CuCrZr pipe during plasma limited configuration with 14MW absorbed power (10MW/m^2 peak heat flux).

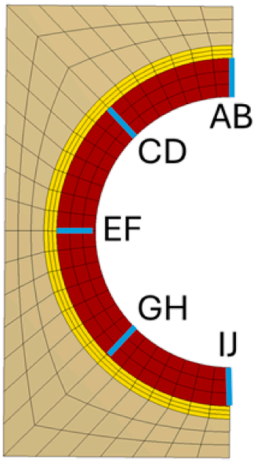

Fig. 12. Detail of the five critical paths considered in the structural assessment of the CuCrZr pipe.

peaked load distribution, the $3S_m$ rule is verified up to a peak heat flux of 6–8MW/m^2. It slightly decreases to 5–7MW/m^2 if the heat flux is applied uniformly along the PFU (Fig. 13b), owing to a small increase of the stress level in the pipe with respect to the previous case. The small stress increase is consistent with the fact that even in the peaked load configuration the maximum heat flux remains constant over an axial length covering at least one entire monoblock (30 mm). As further confirmation, only marginal improvement was noticed by reducing the axial thickness of the monoblocks in the loaded zone or by varying the number and location of the pinned supports.

In Fig. 13c, the same results are shown with respect to the combination of peaked heat load and thinner pipe (1.5 mm instead of 3 mm, but with same outer diameter). Despite the lower thickness, the stress intensity does not change significantly, and the overall effect is a narrower range of the maximum allowable load (5–6MW/m^2). To some extent, this result can be explained by the reduction of the HTC resulting from having increased the inner diameter of the outer pipe at a constant mass flow rate. Therefore, the main benefit of having reduced the thickness is counterbalanced by the overall higher average temperature in the pipe.

For instance, at 10MW/m^2 the maximum temperature at the top of the 1.5mm-thick pipe is 343 °C, thus only 51 °C less than the same scenario with a 3mm-thick pipe (Figure 7). A second effect could be related to the different bending strength offered by a thinner pipe. However, further analysis is needed for a better understanding.

Table 3
Structural assessment results. Critical paths are analyzed at two positions of the loaded zone, respectively at the "peak" heat flux and at the pinned "support".

8MW – peak load 6 MW/m^2					
Position	Path	Max Linearized Stress (MPa)	Tm (°C)	3Sm (MPa)	K
Peak	AB	302.8	250	309	0.98
	CD	212.51	200	330	0.64
	EF	122.6	≤100	369	0.33
	GH	61.5	≤100	369	0.17
	IJ	30.3	≤100	369	0.08
Support	AB	215.4	≤100	369	0.58
	CD	133.4	≤100	369	0.36
	EF	53.89	≤100	369	0.15
	GH	169.1	≤100	369	0.46
	IJ	217.7	≤100	369	0.59
14MW – peak load 10 MW/m^2					
Location	Path	Max Linearized Stress (MPa)	Tm (°C)	3Sm (MPa)	K
Peak	AB	384.3	350	264.4	1.45
	CD	258.0	300	288	0.90
	EF	215.0	150	351	0.61
	GH	141.9	≤100	369	0.38
	IJ	108.8	≤100	369	0.29
Support	AB	320	150	351	0.91
	CD	219.8	≤100	369	0.60
	EF	84.9	≤100	369	0.23
	GH	250.9	≤100	369	0.68
	IJ	320.8	≤100	369	0.87

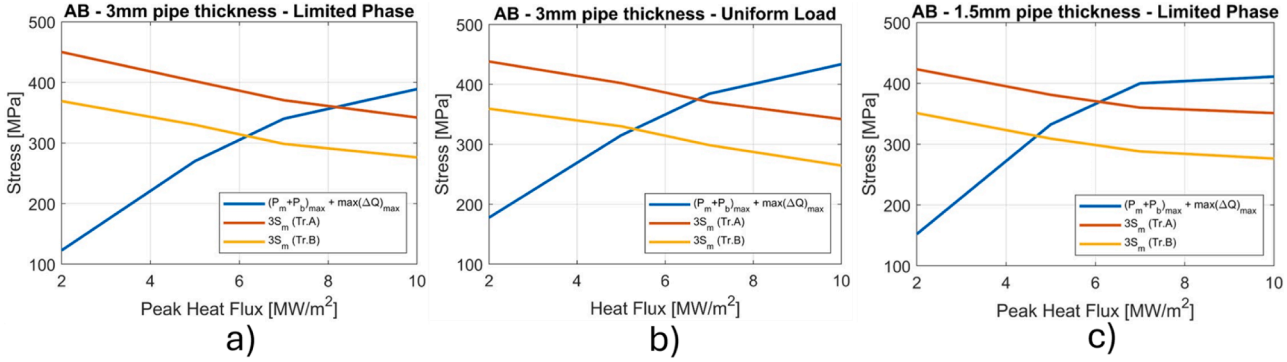

Fig. 13. Results of the PFU structural integrity assessed at the most critical path AB. The 3Sm criterion is verified in the range where the blue curve (max linearized membrane plus bending stress intensity) remains below the 3Sm curves (yellow and orange one depending on the fabrication route of CuCrZr). In graph a) (3mm-thick pipe under peaked heat flux distribution), the upper limit lies in the range 6–8MW/m^2. This limit decreases to 5–7MW/m^2 in graph b), where a uniform load distribution along the PFU is imposed, and it decreases to 5–6MW/m^2 assuming a thinner pipe with a peaked load distribution, as shown in graph c).

5. Conclusions

In support of the ongoing activities aimed at developing the limiter inner first wall of DTT, this paper describes the thermohydraulic and thermo-structural tools developed for the assessment of the technological limits of the LIFW design under conservative but realistic boundary conditions.

First, a MATLAB routine relying on first principles and semi-empirical correlations is described. It provides useful information on the hydraulic limits imposed by the characteristics of the cooling water on the total power that can be absorbed by the LIFW system, having assumed a reasonable safety margin from the critical heat flux.

As a second step, the results of the thermo-structural analyses implemented in ANSYS to assess the behavior and structural integrity of a LIFW unit are described. In addition to a uniform heat load, a parametric wall power density profile can be employed to simulate plasma limited scenarios with loads that can be varied in space and time. For the aim of the present work, such a profile was parametrized with respect to the total power absorbed by the LIFW system, and the structural verification was performed by solving steady state thermal analyses based on the worst instant during a ramp-up phase of DTT. The similations are also relevant for negative triangularity operation as well as for limiter plasma configurations, if foreseen during the commissioning phase. Moreover, realistic kinematic constraints able to accurately reproduce the behavior of the pinned supports are implemented in the finite element code. The structural integrity of the CuCrZr pipe is preliminary verified as prescribed by the ITER SDC-IC elastic analysis approach, thus following a conservative design-by-analysis method. Preliminary results suggest that the maximum peak heat flux that can be handled by the LIFW design lies in the range 5–8MW/m^2.This range is compatible with the DTT "Day0" scenario.

On the other hand, the results at the upper heat load of 10MW/m^2 confirm the need for dedicated high heat flux tests, which are already foreseen for a more accurate lifetime assessment, after the fabrication of small-scale mock-ups. Even if more stringent limitations may arise from the reactor operation, e.g. due to the unacceptable sputtering during limiter operation, the technological limits highlighted in this study provide a preliminary and conservative indication of the operating range of the LIFW design.

CRediT authorship contribution statement

Riccardo De Luca: Writing – original draft, Supervision, Investigation, Formal analysis, Data curation, Conceptualization. **Maurizio Furno Palumbo:** Writing – review & editing, Supervision, Project administration, Conceptualization. **Paolo Frosi:** Writing – review & editing, Validation, Formal analysis, Data curation. **Gabriele De Sano:** Writing – review & editing, Visualization, Methodology, Data curation, Conceptualization. **Matteo Iafrati:** Writing – review & editing, Visualization, Methodology, Investigation. **Gian Mario Polli:** Writing – review & editing, Visualization, Supervision, Resources, Project administration, Funding acquisition. **Bruno Riccardi:** Writing – review & editing, Visualization, Supervision, Project administration, Funding acquisition. **Selanna Roccella:** Writing – review & editing, Visualization, Supervision, Resources, Project administration, Methodology, Funding acquisition, Conceptualization.

Declaration of competing interest

The authors declare that they have no known competing financial interests or personal relationships that could have appeared to influence the work reported in this paper.

Acknowledgements

This work has been carried out within the framework of the EUROfusion Consortium, funded by the European Union via the Euratom Research and Training Program (Grant Agreement No 101052200 – EUROfusion). Views and opinions expressed are however those of the author(s) only and do not necessarily reflect those of the European Union nor the European Commission can be held responsible for them.

Data availability

Data will be made available on request.

References

[1] F.A J.H. Donnè, The European roadmap towards fusion electricity, Philos. Trans. R. Soc. A 377 (2141) (2019) 20, vol.170 432.
[2] F. Romanelli, et al., Divertor Tokamak Test facility project: status of design and implementation, Nucl. Fusion 64 (2024) 112015.
[3] G.F. Matthews, et al., Melt damage to the JET ITER-like Wall and divertor, Phys. Scr. T167 (2016) 014070.
[4] F. Maviglia, et al., Integrated design strategy for EU-DEMO first wall protection from plasma transients, Fusion Eng. Des. 177 (2022) 113067.
[5] M. Iafrati, et al., « *Conceptual design of the top and outboard FW, and inboard FW limiters* », EURO Fusion Final Rep. EFDA_D_2PJ2U5 (2021).
[6] A. Cucchiaro, et al., Conceptual 3D CAD model of the FW with internal cooling system collectors and piping, and fixation systems to the VV, EURO Fusion Final Rep. EFDA_D_2PJ6ZQ (2021).
[7] G. De Sano, et al., Thermo-hydraulic design of the first wall of the DTT facility, IEEE Trans. Plasma Sci. 52 (9) (2024) 3865–3870.
[8] I.T.E.R. Organization, Historical baseline document: appendix A materials design limit data, Approv. Version (2013).
[9] M. Mosceni, et al., Cross-code comparison of the edge codes SOLPS-ITER, SOLEDGE2D and UEDGE in modelling a low-power scenario in the DTT, Nucl. Fusion 62 (2022) 056009.

[10] F. Subba, G. Maddaluno, R. Lombroni, Power Distribution on DTT Wall in Ramp-up and NT Scenarios, Private Communication, 2020.
[11] L. Balbinot, et al., Multi-code estimation of DTT edge transport parameters, Nucl. Mater. Energy 34 (2023) (2024) 101350.
[12] N. Bonanomi, et al., Time-dependent full-radius integrated modeling of the DTT tokamak main plasma scenarios, Nucl. Fusion 65 (2025) 016005.
[13] R.J. Goldston, et al., Heuristic drift-based model of the power scrape-off width in low-gas-puff H-mode tokamaks, Nucl. Fusion 52 (2012) 013009.
[14] A. Scarabosio, et al., Outer target heat fluxes and power decay length scaling in L-mode plasmas at JET and AUG, J. Nucl. Mater. 438 (2013) S426–S430.
[15] A.R. Raffray, et al., Critical heat flux analysis and R&D for the design of the ITER divertor, Fusion Eng. Des. 45 (1999) 377–407.
[16] E. Rabaglino, et al., Prediction of heat transfer in water actively cooled plasma facing components, in: XVIII UIT National Heat Transfer Conference, 2000, pp. 823–834.
[17] M.Furno Palumbo, et al., Status of design and manufacturing qualification activities of the first wall of the divertor tokamak test facility, in: Proceedings of the SOFT2024, submitted to Fusion Engineering and Design, 2025.
[18] J.H. You, et al., High-heat-flux performance limit of tungsten monoblock targets: impact on the armor materials and implications for power exhaust capacity, Nucl. Mater. Energy 33 (2022) 101307.